

Violence in the Dark Ages

Robert J. Thacker^{1,2}, Evan Scannapieco^{3,2}

and

Marc Davis²

¹Department of Physics and Astronomy, McMaster University, 1280 Main St. West, Hamilton, Ontario, L8S 4M1, Canada.

²Department of Astronomy, University of California at Berkeley, Berkeley, CA, 94720.

³Osservatorio Astrofisico di Arcetri, Largo E. Fermi 5, Firenze, Italy.

ABSTRACT

A wide range of observational and theoretical arguments suggest that the universe experienced a period of heating and metal enrichment, most likely from starbursting dwarf galaxies. Using a hydrodynamic simulation we have conducted a detailed theoretical investigation of this epoch at the end of the cosmological “dark ages”. Outflows strip baryons from pre-virialized halos with total masses $\lesssim 10^{10} M_{\odot}$, reducing their number density and the overall star formation rate, while pushing these quantities toward their observed values. We show that the metallicity of $\lesssim 10^{10} M_{\odot}$ objects increases with size, but with a large scatter, reproducing the metallicity-luminosity relation of dwarf galaxies. Galaxies $\gtrsim 10^{10} M_{\odot}$ form with a roughly constant initial metallicity of 10% solar, explaining the observed lack of metal-poor disk stars in these objects. Outflows enrich roughly 20% of the simulation volume, yielding a mean metallicity of 0.3% solar, in agreement with observations of C IV in QSO absorption-line systems.

1. Introduction

An epoch of galaxy outflows is a virtually inevitable consequence of hierarchical structure formation. In such models, subunits merge and accrete mass to form objects of ever-increasing size with a rich substructure. Yet while the sizes of galaxies increase strongly over time, the sizes of the structures within them remain largely fixed. Thus such properties as the scale of associations of O and B stars (McKee & Ostriker 1997) and the energy deposition due to the resulting supernovae (SNe) are likely to be weak functions of the mass of the host galaxy, depending mainly on environmental effects such as the distribution of stellar material, gas, and dust (Omukai 2000). Hence, while the ejecta of conglomerations of Type-II SNe are primarily confined to the interstellar medium in Milky Way size galaxies, they are easily able to escape from the dwarf galaxies whose formation at high-redshift ushered in the first period of intense star formation in the universe. Thus the end of the dark ages, before galaxies formed, is likely to have been accompanied by a potentially drastic change of both the properties of the Intergalactic Medium (IGM) and the evolution of collapsing protogalactic dwarf systems (Scannapieco, Thacker & Davis 2001).

From an observational point of view, the evidence for such an epoch is equally compelling. Analyses of C IV lines in QSO absorption spectra uncover an IGM that has been widely and inhomogeneously enriched by stellar material (Cowie, et al. 1995), and heating from outflows is necessary to avoid overproduction

of the X-ray background (Pen 1999). Such mechanisms are believed to be needed to explain the X-ray luminosity-temperature relation ($L_x : T$) of the hot gas in galaxy clusters, which is widely discrepant with predictions that consider only heating from gravitational collapse (Kaiser 1991). Note that a recent argument by Voit & Bryan (2001) shows that the precise details of outflow heating are comparatively unimportant to the shape of the $L_x : T$ relation (excessively heated gas will float to the edges of a cluster where it is undetectable, further, simulations by Pearce et al. (2000) demonstrate that cooling alone will produce a break in the $L_x : T$ relation). Finally, the starbursting galaxies that form the low-redshift end of this epoch have been detected directly, both in optical and infrared observations (Pettini et al. 2001) at $3 \lesssim z \lesssim 4$, and optical observations (Frye, Broadhurst & Benitez 2002; Hu et al. 2002) of lensed galaxies at $4 \lesssim z \lesssim 6.56$.

Motivated by this wide range of observational evidence and theoretical pointers, we have carried out a detailed numerical study of galaxy outflows, their impact on the IGM, and the formation of galaxies within it. While previously studies of outflows and cosmological metal enrichment have been attempted, these have either employed approximate semi-analytical methods (Nath & Chiba 1995; Madau, Ferrara & Rees 2001; Scannapieco & Broadhurst 2001), low-resolution simulations (Aguirre et al. 2001a; Aguirre et al. 2001b; Cen & Ostriker 1999) that are unable to identify the dwarf galaxies that are likely to be the primary source of metals (Madau et al. 2001; Scannapieco & Broadhurst 2001; Scannapieco, Ferrara & Madau 2002), or a high-resolution scheme in which supernovae explosions were not adequately accounted for (Gnedin & Ostriker 1997). We also conducted an earlier study (Scannapieco et al. 2001) in which we demonstrated that outflows can reduce the number density of dwarf galaxies at high redshift. This effect was seen to be a combination of ‘baryonic stripping’, whereby outflows strip gas from low over-density halos, and a delay in formation times caused by outflows slowing accretion on to the host halo. However, due to the significant wall clock time required to conduct the simulations we were unable to integrate them beyond a redshift of $z = 6$. In this paper we build on our previous work, firstly by improving the physical model through the inclusion of variable metallicity and, secondly, we incorporate a new numerical technique to integrate to a directly observable epoch. By adopting a simple model for outflow generation and enrichment with stellar material in high-resolution cosmological simulations, we demonstrate that the inclusion of winds is able to explain a diverse set of poorly understood properties of objects ranging from moderately-sized galaxies to the absorption clouds that trace the most tenuous cosmological structures.

2. Simulations of Galaxy Outflows

Based on the latest measurements of the Cosmic Microwave Background and the number abundance of galaxy clusters (Balbi et al. 2000; Vianna & Liddle 1996) we focus our attention on a Cold Dark Matter cosmological model with parameters $h = 0.65$, $\Omega_0 = 0.35$, $\Omega_\Lambda = 0.65$, $\Omega_b = 0.05$, $\sigma_8 = 0.87$, and $n = 1$, where h is the Hubble constant in units of $100 \text{ km s}^{-1} \text{ Mpc}^{-1}$, Ω_0 , Ω_Λ , and Ω_b are the total matter, vacuum, and baryonic densities in units of the critical density, σ_8^2 is the variance of linear fluctuations on the $8h^{-1}\text{Mpc}$ scale, and n is the “tilt” of the primordial power spectrum.

As in our earlier work (Scannapieco et al. 2001), simulations were conducted with a parallel OpenMP based implementation of the “HYDRA” code (Thacker & Couchman 2000) that uses the Adaptive Particle-Particle, Particle-Mesh algorithm (Couchman 1991) to calculate gravitational forces, and the Smoothed Particle Hydrodynamic (SPH) method (Lucy 1977; Gingold & Monaghan 1977) to calculate gas forces. We simulate a periodic box of size $5.2 h^{-1}$ comoving Mpc containing 192^3 dark matter and 192^3 gas particles with masses of $2.5 \times 10^6 M_\odot$ and $5.0 \times 10^5 M_\odot$ respectively. This is sufficient to resolve the

smallest objects that are able to cool efficiently without molecular hydrogen, with masses $\gtrsim 10^8 M_\odot$. We chose this limit as primordial molecular hydrogen is extremely fragile, and is likely to be quickly dissociated by the first stars that form at very high redshift (Haiman, Rees & Loeb 1997). Note that while alternative schemes for creating cosmological H_2 have been suggested, star formation and outflow generation is likely to be inefficient in objects that rely on molecular cooling, causing them to have a small overall impact on IGM heating and enrichment (Madau et al. 2001; Scannapieco et al. 2002). Forces are softened using a fixed physical Plummer softening length of 1.54 kpc, yielding a minimum hydrodynamic resolution of 1.8 kpc; gas densities and energies are calculated using the standard SPH smoothing kernel method (Scannapieco et al. 2001), with the kernel tuned to smooth over 52 particles; and radiative cooling is calculated using standard tables (Sutherland & Dopita 1993). Because the epoch of reionization is unknown, and also for reasons of simplicity, we do not include a fiducial photoionization background in the simulation.

Under heavy particle clustering, and when implemented with a minimum resolution limit, the SPH method can degenerate to an order N^2 algorithm. While some authors resort to merging particles to avoid this problem, this breaks the one-to-one relationship between mass and particle number and leads to a degradation of accuracy in the hydrodynamic calculation. Our solution to this problem (Thacker 2002) is to calculate an aggregate solution in regions below the resolution limit, grouping particles in sets of 4-30 that may change from step to step, while never actually merging particles together. The errors introduced by this method are far smaller than those created by merging particles, and the algorithm remains less than order $N^{3/2}$ under heavy clustering, which translates to a three-fold performance improvement over our previous code (Scannapieco et al. 2001).

To study the propagation of galaxy outflows, it is first necessary to identify where galaxies are forming. Typically, this is done using the friends-of-friends group finding algorithm which relies upon calculating inter-neighbor distances (Efstathiou et al. 1985), however this technique is very computationally expensive. We therefore adopt an alternative approach in which we search for regions where gas particles exceed a density threshold δ_c times the mean gas density. Provided more than $2.6 \times 10^7 M_\odot$ (our effective mass resolution limit) is contained in such a region, the object is counted as a galaxy. This method performs well in comparison to the friends-of-friends technique (Scannapieco et al. 2001), and throughout this paper we set $\delta_c = 500$.

Star formation is modeled by converting a fixed fraction, $\epsilon_{sf} = 0.1$, of the gas in a collapsed object into stars in a single starburst. Subsequent starbursts within a galaxy are likely to be smaller and less efficient, so our model is a conservative lower limit on star formation activity. The gas involved in a starburst is tagged to prevent further bursts until a sufficiently large reservoir of ‘fresh’ gas is accumulated. Star formation can only occur when over one-third of the galaxy, and at least 52 new particles, are untagged, although testing has shown that these thresholds can be varied over a wide range with only a small effect on our results (Scannapieco et al. 2001). Finally, we also impose an upper limit of 1000 particles per burst, corresponding to $5 \times 10^8 M_\odot$ of stars, which prevents unphysically large groups of supernovae from exploding simultaneously and generating enormous outflows (Ferrara, Pettini & Shchekinov 2000).

The structure of galaxy outflows has been studied in detail previously (Mac Low & Ferrara 1999; Martel & Shapiro 2000; Mori, Ferrara & Madau 2001), yielding the conclusion that in starbursting disk galaxies with masses $\lesssim 10^{10} M_\odot$ “blow-out” occurs. In these galaxies, the superbubbles around groups of Type-II SNe punch out of the plane of the disk and shock the surrounding IGM although they fail to excavate the interstellar medium itself. Guided by this scenario, we model the sub-resolution physics of outflow generation by rearranging the IGM surrounding a galaxy while leaving the central object intact.

Hence we construct our outflows from gas particles within a radius twice that of the central galaxy ($r \leq 2r_g$), but outside the galaxy itself ($r > r_g$). This local IGM is arranged randomly into two concentric spherical shells of radius $2.0r_g$ and $1.8r_g$ of equal mass. This multi-shell structure assures that the outflows will be sufficiently well-resolved radially to be reasonably treated by the SPH algorithm. Sufficient resolution in each of the shells is assured by arranging the particles in an anti-correlated fashion such that all particles have an inter-neighbor distance in excess of half the average inter-particle spacing. We have tested this approach in detail against one-dimensional analytical models of expanding shells, and have found that it reproduces these results almost exactly (Scannapieco et al. 2001).

The particles in these shells are assigned velocities that conserve their overall center of mass velocity and angular momentum, and include a velocity boost in the radial direction. The strength of this boost is determined by assuming that a fixed fraction of the mechanical energy from supernovae from each starburst is channeled into the outflow, $\epsilon_{\text{wind}} = 0.1$. We estimate this kinetic input to be 2×10^{51} ergs per supernova, to take into account the contribution from stellar winds, and assume that one supernova occurs for every $100 M_\odot$ of stars formed (Gibson 1997).

Our previous simulations side-stepped the issue of metal enrichment, taking a fixed value of $0.05 Z_\odot$ for all gas particles. In this work we adopt a more realistic model in which the primordial metallicity is taken to be zero, and gas particles are enriched by ejecta from Type-II SNe. The metal content of each gas particle is therefore allowed to evolve in a similar fashion to hydrodynamic variables. We assume a standard yield of $2 M_\odot$ of metals per SNe, corresponding to an effective metal yield $p = 0.02$, and distribute this material equally between the galaxy and the outflow. For these parameters a galaxy will be enriched following the first outflow event to a metallicity Z_{gal} given by, $\log_{10}(Z_{\text{gal}}/Z_\odot) \sim \log_{10}(\epsilon_{\text{sf}} \times f \times p/Z_\odot) = -1.3$, if we take $f = 0.5$ as the fraction of metals retained by the galaxy. Following an outflow event, the total metal yield, by mass, for the galaxy is distributed evenly among gas particles that determined to be in the galaxy ($\delta M_{\text{particle}}^Z = (1/N_{\text{gal}})f M_{\text{total}}^Z$, where M_{total}^Z is the total metal yield, by mass, of the starburst, N_{gal} is the number of particles in the galaxy and $\delta M_{\text{particle}}^Z$ is the increase in the metal mass of a particle in the galaxy). Similarly, the metal yield deposited in the outflow is distributed evenly among gas particles determined to be in the outflow ($\delta M_{\text{particle}}^Z = (1/N_{\text{outflow}})(1 - f) M_{\text{total}}^Z$). Individual gas particles can undergo multiple episodes of enrichment in response to a series of outflows.

Enriched particles retain their metals for the remainder of the simulation, and the spatial metal distribution is calculated by convolving with the SPH smoothing kernel. The smoothed field is then used self-consistently in computing gas cooling. This may be viewed as assuming the metals within a given particle’s smoothing length are well mixed, a reasonable approximation given that the Rayleigh-Taylor instability will mix gases in a time roughly proportional to the size of the region divided by the sound speed.

3. Outflows and Structure Formation

We have conducted two simulations: a fiducial run in which we fix the star-formation and outflow efficiencies to be $\epsilon_{\text{sf}} = \epsilon_{\text{wind}} = 0.1$, and a comparison “no-outflows run” in which we fix $\epsilon_{\text{sf}} = 0.1$ but do not include metal enrichment or outflows. In the fiducial run the gas is initially free of metals, while in the no-outflows run the metallicity is fixed at $0.05 Z_\odot$ at all times. While particle-particle interactions halted our previous simulations at $z = 6$, the pseudo-merging scheme discussed above allowed us to reach $z = 4$ in this study. A total of 4515 outflows were generated in this case, with initial radial velocities ranging from 80 to 300 km/s, consistent with direct observations (Pettini et al. 2001; Frye, Broadhurst & Benitez 2002).

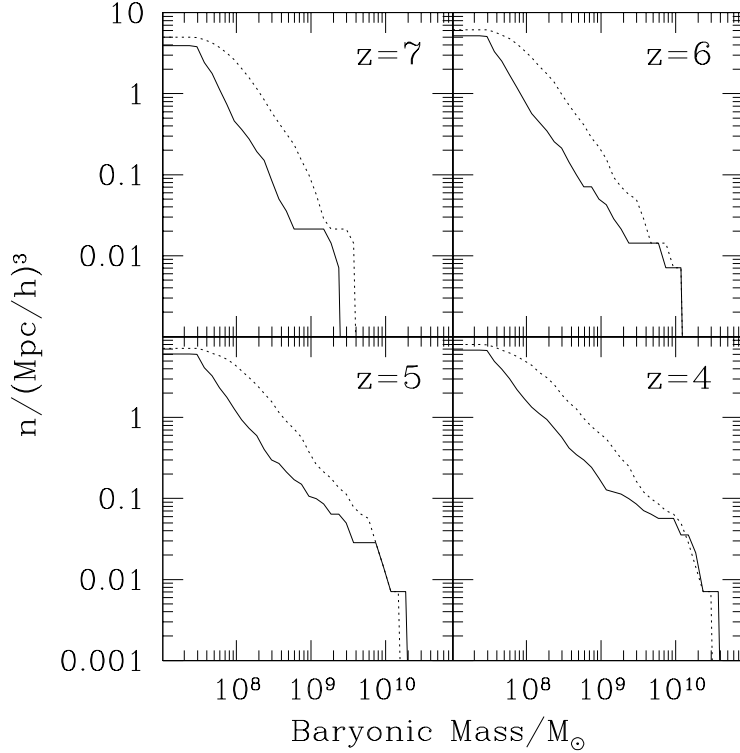


Fig. 1.— Number density of galaxies as a function of their baryonic mass. Redshift is given in the upper right corner of each panel, the solid lines are from the simulation with outflows, and the dotted lines are from the star-formation only simulation.

The cumulative number density of galaxies within the simulations as a function of baryonic mass and redshift is shown in Figure 1. Below a limiting mass of $5 \times 10^9 M_\odot$, two significant features are observed. Firstly, there is an overall reduction in the baryonic mass of the objects in the outflows run. This is caused by outflows suppressing accretion onto the host galaxy, a process that is similar to that described in earlier work (Dekel & Silk 1986) on dwarf galaxies which showed that supernova-driven winds result in a systematic bias toward higher mass-to-light ratios. Secondly, the fiducial run also contains many examples of the “baryonic stripping” mechanism previously identified (Scannapieco, Ferrara & Broadhurst 2000). In these cases, the momentum in an outflow is sufficient to evacuate gas from nearby overdense regions that would have otherwise later formed into dwarf galaxies, leaving behind empty ‘dark halos’ of cold dark matter. Note also that this overall suppression of objects points to a possible solution to the discrepancy between the number of local group dwarf galaxies and predictions from CDM models that do not include outflows (Klypin et al. 1999).

Above $\gtrsim 5 \times 10^9 M_\odot$, the number-densities in the two models become similar, which was not observed in our previous work (Scannapieco et al. 2001). Thus this feature may be related to the key difference between these simulations: the inclusion of gas enrichment by supernovae. To study this further, we plot the mean metallicity of the gas particles identified in galaxies as a function of galaxy mass in Figure 2A. Here we see that above $\sim 10^9 M_\odot$, the metallicity is roughly constant at $0.1 Z_\odot$. While our models do not include the quiescent mode of star formation that is important in such large objects, this value is suggestive of the $\sim 0.1 Z_\odot$ pre-enrichment necessary to explain the lack of low-metallicity G dwarf stars in the solar

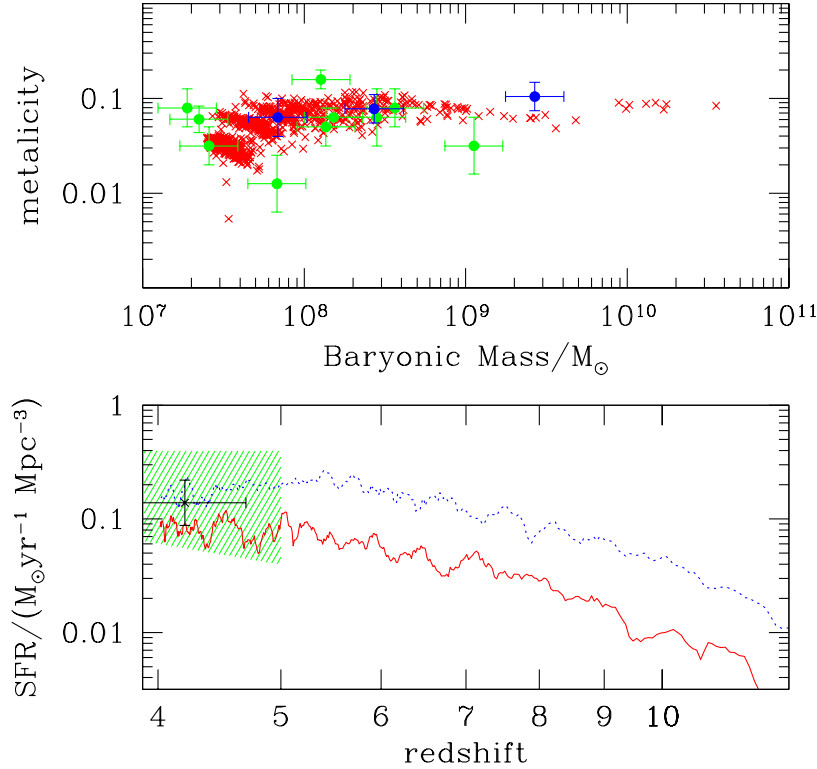


Fig. 2.— **(A)** Mean metallicity of gas particles within each galaxy as a function of its total baryonic mass, at a fixed redshift $z = 4$ (crosses). Here the solid points are local group dwarves (Mateo 1998) shifted by a constant factor of Ω_b/Ω_0 . The green points represent observations of iron abundances, while the blue points represent objects for which only the oxygen abundance has been measured. **(B)** The star formation rate as a function of redshift. The solid lines and dotted lines correspond to the fiducial and no-outflows case respectively. The data point is taken from observations (Steidel et al. 1999) and the green region is a compilation of indirect constraints (Hopkins et al. 2001).

neighborhood (Ostriker & Thuan 1975), as well as in other large nearby galaxies (Thomas, Greggio & Bender 1999), a result that is consistent with semi-analytic studies (Scannapieco & Broadhurst 2001).

Using a simple estimate for the “cooling time” (see Scannapieco & Broadhurst 2001) we can get a rough idea of the delay between gas collapse and cooling into a disk for the large objects in these simulations, which is a strong function of metallicity. Referring to Figure 1, we see that above $2 \times 10^{10} M_{\odot} \Omega_0/\Omega_b$ the enrichment run appears to contain more massive galaxies than the non-enrichment run, although there are only two halos in the simulation that are above this threshold and we would prefer better statistics before making definitive conclusions. For the sake of reference we call this mass threshold the ‘crossover’ mass. We note that there was no evidence for a crossover phenomenon in our previous simulation work (Scannapieco et al. 2001).

For galaxies with total masses roughly corresponding to the crossover value the cooling time is $\sim 3.0 \times 10^8$ years for $0.05 Z_{\odot}$ metallicity gas and 1.5×10^8 years for gas at $0.1 Z_{\odot}$ metallicity. Comparing these values with the age of the universe in this cosmology (11.5×10^8 years at $z = 5$ and 14.8×10^8 years at $z = 4$) shows that approximately 3.3×10^8 years passes between $z = 4$ and $z = 5$, which is very

slightly larger than the cooling time for the $0.05 Z_{\odot}$ gas, and about twice the cooling time of the $0.1 Z_{\odot}$ gas. Both of these cooling times are significantly shorter than the Hubble time at $z = 4$ which implies that the increased cooling rate can only have an effect on halo gas that is close to the galaxy. Given the small mass fraction of this gas it seems somewhat unlikely that it would contribute to such a noticeable mass increase. An alternative explanation may be that massive halos act as a sink for outflow material from surrounding smaller systems. However, if this were the case we would expect to have seen the effect of this in Scannapieco et al. (2001). Ultimately, an exact determination of the nature of the apparent increase in mass requires a larger simulation box to improve statistics.

Our outflow model also has important implications for galaxies with baryonic masses less than $10^9 M_{\odot}$, whose metallicities range from $0.02 Z_{\odot}$ to $0.1 Z_{\odot}$ in our simulations. This distribution can be compared with metallicities observed in local group dwarf galaxies, which are thought to form at high redshift. To facilitate this comparison, we overplot in Figure 2A the masses and metallicities of these objects as compiled in a review of the local group galaxies (Mateo 1998), using the iron abundances when available, and assuming a “shifted” solar abundance of $10^{9.4}$ in cases in which only the oxygen abundance was measured. Note that this standard shift is also taken in the observational literature (Mateo 1998) because these objects are rich in α elements such as oxygen, which are abundant in the type-II SNe such as those driving our outflows. In each case we assume a standard error in the mass determination of 50%, due to errors in determining the velocity dispersion and distance to these objects, and apply an overall mass shift of Ω_b/Ω_0 . Clearly our model does a good job of reproducing the metallicity-luminosity relation seen in dwarf galaxies, in which metallicity increases as a function of luminosity, but with a scatter of almost an order of magnitude.

Compared to the enrichment values presented in Gnedin & Ostriker (1997) our values are lower, by an approximate factor of 3-4, in the highest density regions. Most of this difference is probably attributable to the difference between the star formation rates, as the inclusion of outflows systematically lowers our SFR (although we lack a photoionization background). We also have significantly less scatter in the observed metal fractions, which is a function of differences between the numerical methods employed. Gnedin & Ostriker adapt the method presented in Cen & Ostriker (1992) which involves converting mass in cells obeying overdensity, cooling and convergence criteria to collisionless stellar particles. This can lead to a widely varying enrichment history depending upon the details of the density of the gas in the protogalaxy. In our model we ignore the inner structure of our halos and instead treat them as uniform systems that undergo global starbursts when sufficient gas has been accumulated, as is done in semi-analytic models. In passing, we mention that our results for protogalaxy metallicity show good agreement with averaged enrichment values presented in Cen & Ostriker (1999), provided that a log-linear extrapolation to $z=4$ is reasonable.

Despite the increased formation of large objects in the outflows simulation, their comparative rarity at these redshifts causes the total amount of cooled gas to be dominated by the suppression effect. In Figure 2B we plot the overall star formation rate (SFR) as a function of redshift in each of these simulations. The plot shows that the inclusion of outflows results in a decrease in the SFR by approximately a factor of two. We also compare the calculated SFRs with direct observations of star formation (Steidel et al. 1999) and a broad range of indirect constraints (Hopkins et al. 2001). While both models are consistent with the indirect constraints, the direct observations are slightly over-predicted by the no-outflows run and slightly under-predicted in the fiducial run. As our starburst model does not include the quiescent mode of star formation, our results should be considered lower limits on the global SFR. Thus, although the data seems to favor the fiducial run, no definitive conclusions can be drawn.

It is worth noting that the star formation rate only becomes significant at redshifts $\lesssim 10$. This redshift

is determined by the minimum mass scale in our simulations, chosen to be the minimum mass that can cool effectively without molecular hydrogen, which we assume to be completely dissociated.

We have not included a photoionization background in our simulation primarily because we wanted to observe the effect of the outflow model without having to disentangle it from other physical phenomena. Nonetheless, it is important to assess what effect the inclusion of photoionization field might have. Photoionization is known to reduce the number density of dwarf systems, and is considered to be the primary solution to the ‘substructure problem’ (Klypin et al. 1999; Moore et al. 1999). Most simulations of photoionization have concentrated on either large scales with a comparatively low mass resolution (eg Katz et al. 1996) or very small scales at high mass resolution to examine phenomenology of individual halos (eg Navarro & Steinmetz 1997). On the other hand semi-analytic studies are able to provide both good statistics and high mass resolution (eg Somerville 2002), at the cost of lost geometric information and highly phenomenological physics.

Our minimum halo mass resolution is slightly under $1.5 \times 10^8 M_\odot$. At this mass scale the $z = 0$ V-band luminosity function for the semi-analytic model of Somerville (2002) is about a factor of three times lower when a photoionization background is included. This result is surprisingly insensitive to the actual photoionization epoch, and large differences between different photoionizing models are only found at mass scales that we do not resolve (around $10^7 M_\odot$, i.e. close to the mass of the Draco dwarf spheroidal). Thus, assuming that not all dwarf systems are late forming, we can expect our simulation to over-predict the number of dwarf halos by at most a factor of three. The natural effect of a reduced number density of gaseous halos is a reduced global SFR and reduced enrichment volume factor, although the metallicity values for individual galaxies will be similar. However, in all likelihood, some of the protogalaxies that are destroyed by outflows would be suppressed, or possibly erased, by a photoionization background. Thus an accurate assessment of the effect of a photoionization background on the outflow model is quite difficult. Also if the epoch of reionization is optimistically late ($z \sim 7$), then we can expect a less significant impact on our model, as a large amount of the evolution will occur without the presence of a photoionizing background. In this case the SFR at $z = 7$ will undoubtedly plateau, or turn off somewhat, and the enrichment fractions will be reduced. Ultimately, determining the precise impact of a photoionization background requires running a self consistent simulation that includes it.

4. Outflows and the Intergalactic Medium

The widespread generation of outflows has an impact over regions much larger than the dense peaks identified as galaxies. Indeed the strongest inference of an epoch of galaxy outflows is drawn from observations of the IGM itself.

There are two methods by which this impact can be quantified. The first of these is by examining the overall mass of gas enriched by stellar material, which we plot as a function of redshift in Figure 3A. While outflows vigorously enrich the densest regions, the IGM transition associated with outflows is incomplete, and only $\sim 20\%$ of the particles are enriched by redshift 4. In this plot we also see that the majority of enrichment takes place at redshifts below 10, when atomic transitions become an effective coolant.

The onset of this enrichment roughly corresponds with the sharp rise in the number of outflows at $z > 10$, as shown in Figure 3B. This plot, which displays the outflow rate per unit Mpc^3 per Gyr, also hints at the end of the epoch of galaxy outflows as the curve begins to turn over at lower redshift values. The details of this turn-over are quite uncertain, however, and model dependent. The determining factor in

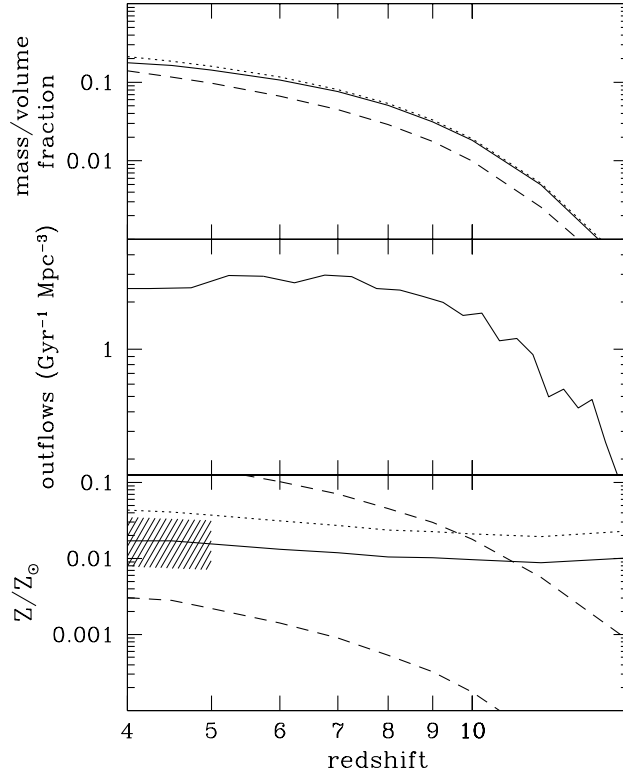


Fig. 3.— **(A)** Fraction of gas particles enriched by outflows as a function of redshift. Here the solid lines represent the mass fraction of particles that are *not* labeled as belonging to galaxies, while the dotted lines include all enriched gas particles. Finally, the dashed line gives that volume fraction enriched to $0.0001 Z_{\odot}$ or greater. **(B)** Outflows rate per unit volume as a function of redshift. **(C)** Mean metallicity of enriched particles as a function of redshift. Solid and dotted lines are as in A, while the dashed line is an average over all gas particles in the simulation, not tagged as galaxies. The green region shows the range of metallicities for the gas within galaxies as calculated in earlier analytic models (Pei, Fall & Hauser 1999).

this case is the maximum size of the gravitational potential from which SNe can successfully cooperate to drive a large-scale outflow, a quantity that is crudely modeled by our overall upper limit of 1000 particles. In reality this turn-over is dependent on such uncertain quantities as the distribution of high-redshift OB associations, the star formation efficiency, and the stellar initial mass function in high-redshift galaxies (Mori et al. 2001).

In Figure 3C we examine the overall level of enrichment within the affected regions, and also plot the bounds from analytic models (Pei, Fall & Hauser 1999) for reference. The slight decrease in these values seen at large redshifts is likely to be due to low-number statistics, as only ~ 15 objects are formed in this simulation by $z = 15$. Despite the fact that outflows are able to enrich the largest objects to metallicities of $\sim 0.1 Z_{\odot}$, their mean impact on polluted regions of the IGM is only on the order of $0.02 Z_{\odot}$, and the mean value when averaged over the simulation as a whole is $0.003 Z_{\odot}$. Thus our model not only results in a patchy distribution of enriched regions, but also a large variance within these regions. This is consistent with observations of C IV at $z \approx 3$ in QSO absorption systems, which can be reproduced by a model in which the overall mean metallicity of the IGM is $0.003 Z_{\odot}$ with a large scatter of roughly an order of magnitude

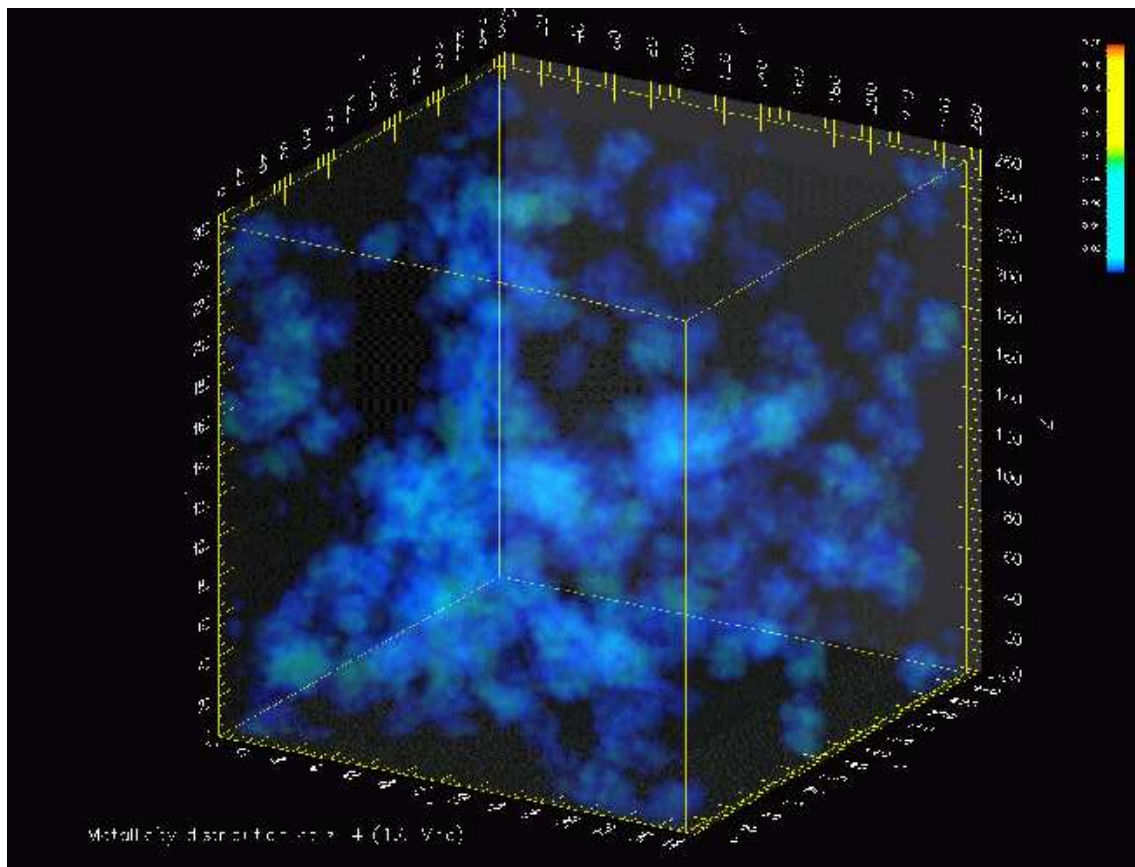


Fig. 4.— Volume-rendered image of metal enrichment at $z = 4$. (Full resolution version available from coho.mcmaster.ca/~thacker/fig4.eps.gz.)

(Hellsten et al. 1997).

To get a better handle on this inhomogeneity, we turn our attention to the second method of quantifying this IGM transition and examine the volume impacted by outflows. Figure 4 is a volume-rendered image of the smoothed distribution of metals in our simulation volume. Here we see that the spatial distribution of material from outflows is highly biased, illustrating the necessity of studying this problem through simulations or other techniques that capture this inhomogeneity (Scannapieco & Broadhurst 2001). While much of the simulation remains metal free, large clouds of $\sim 0.02 Z_{\odot}$ material roughly outline the underlying filaments of dark matter, punctuated by smaller regions of higher metallicity.

In Figure 3A we plot the redshift evolution of the volume enriched to $0.001Z_{\odot}$ or greater. The volume fraction enriched follows the trend of the mass enriched but is reduced because of the large overdensities at which galaxies form. To quantify this further, in Figure 5 we plot the volume filling factor of material with metallicity above a given threshold value, plotted as a function of the threshold value at $z = 4$. At this redshift the maximum enrichment volume is slightly over 20%, consistent with new semi-analytic calculations (Scannapieco et al. 2002), and apparently at odds with the claimed (Madau et al. 2001) 100% value for $z = 10$.

While Madau, Ferrara, & Rees (2001) only considered outflows from objects at a fixed mass scale of of

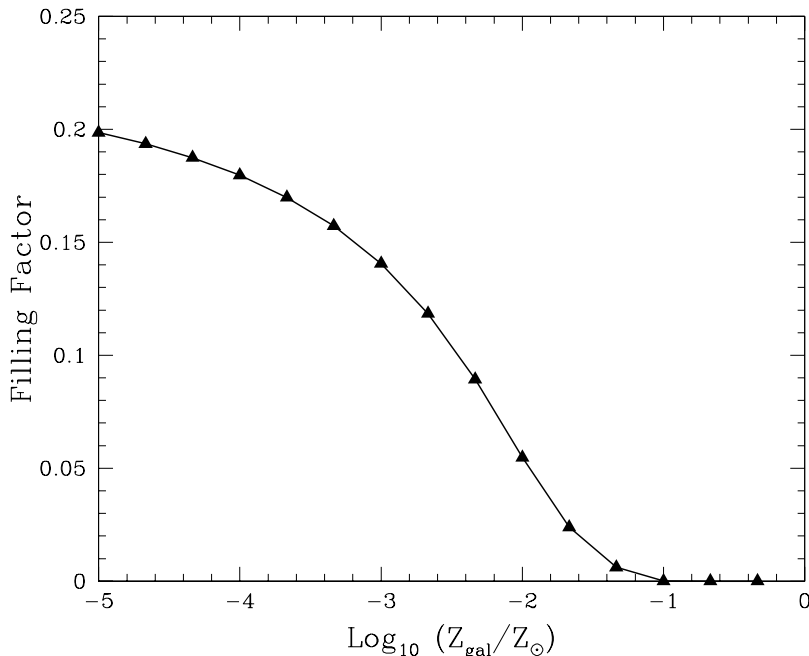


Fig. 5.— Volume filling factor of enriched material with metallicity values above a given threshold, plotted as a function of threshold at $z = 4$.

$10^8 M_{\odot}/h$ and then multiplied by a Press-Schechter estimate of their number density to compute the overall filling factor, the overall energetics of their wind models are quite similar to ours. Thus it is likely that the primary source of this inconsistency is related instead to their adoption of an sCDM cosmology with parameters $\Omega_m = 1$, $h = 0.5$, $\sigma_8 = 0.63$, $n = 1$, $\Omega_b h^2 = 0.019$. Indeed, using the standard Press-Schechter approach to calculate the comoving number density of halos of masses greater than $10^8 M_{\odot}/h$ at $z = 9$ we find that the sCDM model of Madau, Ferrara & Rees (2001) contains 5.5 times as many objects per $\text{Mpc } h^{-1}$ as our Λ CDM model. This enhancement is primarily due to the association of a smaller top-hat filtering scale to sCDM objects as compared with their $\Omega_M = 0.35$ counterparts, and is sufficient to explain the factor of 5 difference that we observe between our results. We therefore conclude that the difference between filling factors can be attributed almost entirely to the reduced number counts of dwarf galaxies in the observationally motivated Λ CDM cosmology compared to the out of favor sCDM model.

Nonetheless, Figure 5 clearly shows that enrichment is far from uniform. Metallicities greater than $0.01 Z_{\odot}$ are confined to less than 5.5% of the volume, while enrichments in excess of $0.1 Z_{\odot}$ are confined primarily to larger dwarf galaxies and their halos, which occupy less than 0.1% of the simulation volume. This correlation between the distribution of metals and starbursting galaxies provides a natural explanation for a long standing dichotomy seen in QSO absorption line studies. For while it is clear that the distribution of $\text{Ly}\alpha$ in the IGM as a whole is well modeled without considering outflows (McDonald et al. 2000), studies of C IV clouds indicate that these enriched objects have been turbulently stirred by events occurring on timescales on the order of 10^8 years (Rauch et al. 2000).

5. Conclusion

In this work, we have studied the role of outflows and metal enrichment in structure formation, comparing our results to a diverse set of observations. We have not attempted to calculate the properties of individual galaxies, but rather have used results from previous studies as input into our model. While based on the approach described in Scannapieco, Thacker, & Davis (2001), this study is a significant advance over our previous work as it includes a more realistic model of metal enrichment as well as a more efficient SPH algorithm that allows us to integrate to directly observable redshifts. This leads to a number of important conclusions, which merit further investigation.

First, while the presence of outflows greatly reduces the number of galaxies formed at lower mass scales as a result of baryonic stripping, this mechanism is effective only for galaxies with total mass below $5 \times 10^9 M_\odot$. At greater mass scales, the galaxy number counts in the outflows case become similar or even exceed that of the no-outflows case as a result of more rapid cooling caused by metal enrichment.

Second, the inhomogeneous distribution of metals by outflows leads naturally to a scatter in metallicity of lower mass objects that is consistent with observations of local group dwarf galaxies. Above $10^9 M_\odot$, however, the metallicity is roughly constant at $0.1 Z_\odot$ in agreement with pre-enrichment estimates necessary to explain the lack of low-metallicity G-dwarf stars in the solar neighborhood.

Third, the global SFR for our model is in broad agreement with observations, albeit on the low side. This is attributed to the lack of quiescent star formation in our model.

Finally, our global enrichment value of $0.3\% Z_\odot$ is consistent with observations of C IV at $z \simeq 3$ in QSO absorption systems. This metal enrichment is far from uniform and concurs with the interpretation that C IV clouds are turbulently stirred on small scales while the distribution of Ly α clouds remains comparatively unaffected.

Future work needs to address the role of H₂ cooling in our simulations as at the moment we make no attempt to calculate production of H₂. Progress is difficult on this front as while calculation of rate equations is comparatively straightforward (and has been conducted within in our simulation framework, see Fuller & Couchman 2000) a fully consistent solution with local photodissociation is, at least at the moment, an extreme computational challenge (eg Razoumov & Scott 1999). We also plan to include the fiducial photoionization background associated with the epoch of reionization. We will address both of these issues over the coming months, although we do not anticipate a major revision of our current results.

We thank Andrea Ferrara, Tom Broadhurst and Mordecai Mac Low for helpful discussions, Greg Bryan for making available unpublished results and the anonymous referee for suggesting a number of changes that significantly improved the content of the paper. We also gratefully acknowledge the hospitality of Carlos Frenk and the Physics Department at the University of Durham where this paper was finished. E.S. has been funded in part by an NSF MPS-DRF fellowship. R.J.T. acknowledges funding from the Canadian Computational Cosmology Consortium and NSERC of Canada via the operating grant of Prof H. M. P. Couchman. This project was supported by NSF KDI grant 9872979.

REFERENCES

Aguirre, A., Hernquist, L., Schaye, J., Weinberg, D. H., Katz, N., & Gardiner, J., 2001, ApJ, 560, 599

- Aguirre, A., Hernquist, L., Schaye, J., Katz, N., Weinberg, D. H., & Gardiner, J. 2001, *ApJ*, 561, 521
- Balbi, A. et al. , 2000, *ApJ*, 545, L1
- Cen, R. & Ostriker J. P., 1999, *ApJ*, 519, L109
- Couchman, H. M. P., 1991, *ApJ*, 386, L23
- Cowie, L.L., Songaila, A., Kim, T. S., & Hu, 1995, *AJ*, 109, 1522
- Dekel, A. & Silk, J., 1986, *ApJ*, 303, 39
- Efstathiou, G., Davis, M., Frenk, C. S., & White, S. D. M., 1985, *ApJS*, 57, 241
- Ferrara, A., Pettini, M. & Shchekinov, Y., 2000, *MNRAS*, 319, 539
- Frye, B., Broadhurst, T. & Benitez, N., 2002, *ApJ*, 568, 558
- Fuller, T., & Couchman, H. M. P., 2000, *ApJ*, 544, 6
- Gibson, B. K., 1997, *MNRAS*, 290, 471
- Gingold, R. A. & Monaghan, J. J., 1977, *MNRAS*, 181, 375
- Gnedin, N. Y. & Ostriker J. P., 1997, *ApJ*, 486, 581
- Haiman, Z., Rees, M. & Loeb, A., 1997, *ApJ*, 476, 458 *erratum* **484**, 985 (1997)
- Hellsten, U., Davé, R., Hernquist, L., Weinberg, D. H. & Katz, N., 1997, *ApJ*, 487, 482
- Hopkins, A. M., Irwin, M. J. & Connolly, A. J., 2001, *ApJ*, 558, L31
- Hu, E. M., et al. , 2002, *ApJ*, 568, L75
- Kaiser, N., 1991, *ApJ*, 383, 104
- Katz, N., Weinberg, D. H., Hernquist, L. & Miralda-Escude, J., 1996, *ApJ*, 457, L57
- Klypin, A., Kravtsov, A. V., Valenzuela, O. & Prada, F., 1999, *ApJ*, 522, 82
- Lucy, L. B., 1977, *AJ*, 82, 1013
- Mac Low, M. M., & Ferrara, A., 1999, *ApJ*, 513, 142
- Madau, P., Ferrara, A. & Rees, M. J., *ApJ*, 555, 92
- Martel, H. & Shapiro, P. R., 2000, in *The Seventh Texas-Mexico Conference on Astrophysics: Flows, Blows, and Glows*, ed. W. Lee & S. Torres-Peimbert, *RevMexAA (Serie de Conferencias)*
- Mateo, M., 1998, *Annu. Rev. Astron. Astrophys.* , 36, 435
- McDonald, P., Miralda-Escudé, J., Rauch, M., Sargent, W. L. W., Barlow, T. A.; Cen, R. & Ostriker, J. P., 2000, *ApJ*, 543, 1
- McKee, C. F., & Williams, J. P., 1997, *ApJ*, 476, 144
- Moore, B., Ghigna, F., Governato, F., Lake, G., Stadel, J. & Tozzi, P., 1999, *ApJ*, 524, L19

- Mori, M., Ferrara, A., & Madau P., 2001, ApJ accepted, available at xxx.lanl.gov/abs/astro-ph/0106107
- Nagataki, S. & Sato, K., 1998, ApJ, 504, 629
- Nath, B. & Chiba, M., 1995, ApJ, 454, 604
- Navarro, J. F. & Steinmetz, M., 1997, ApJ, 478, 13
- Omukai, K., 2000, ApJ, 534, 809
- Ostriker, J. P. & Thuan, T. X., 1975, ApJ, 202, 353
- Pearce, F. R., Thomas, P. A., Couchman, H. M. P., & Edge, A. C., 2000, MNRAS, 317, 1029
- Pei, Y. C., Fall, S. M. & Hauser, M. G., 1999, ApJ, 522, 604
- Pen, U-L., 1999, ApJ, 510, L1
- Pettini, M. et al., 2001, ApJ 554, 981
- Rauch, M., Sargent, W. L. W., Barlow, T. A. & Carswell, R. F., 2001, ApJ, 562, 76
- Razoumov, A. O., & Scott, D., 1999, MNRAS, 309, 287
- Scannapieco, E. & Broadhurst, T., 2001, ApJ, 549, 28
- Scannapieco, E., Ferrara, A., & Broadhurst, T., 2000, ApJ, 536, L11
- Scannapieco, E., Ferrara, A., & Madau, P., 2002, ApJ submitted, available at xxx.lanl.gov/abs/astro-ph/0201463
- Scannapieco, E., Thacker, R. J. & Davis, M., 2001, ApJ, 557, 605
- Sommerville, R., 2002, ApJ, 572, L23
- Steidel, C. C., Adelberger, K.A., Giavalisco, M., Dickinson, M. & Pettini, M., 1999, ApJ, 519, 1
- Sutherland, R. S., & Dopita, M. A., 1993, ApJS, 88, 253
- Thacker, R. J., in preparation (2002)
- Thacker, R. J. & Couchman, H. M. P., 2000, ApJ, 545, 728
- Thomas, D., Greggio, L. & Bender, R., 1999, MNRAS, 281, 537
- Viana, P. T. P. & Liddle, A., 1996, MNRAS, 281, 323
- Voit, M. G., & Bryan, G., 2001, Nature, 414, 425